Solid-State Fluorescence

DOI: 10.1002/ange.200905428

Strong Two-Photon Excited Fluorescence and Stimulated Emission from an Organic Single Crystal of an Oligo(Phenylene Vinylene)**

Fei Gao, Qing Liao, Zhen-Zhen Xu, Yong-Hao Yue, Qiang Wang, Hao-Li Zhang, and Hong-Bing Fu**

Highly conjugated linear molecules such as poly(phenylene vinylene)s (PPVs) and oligo(phenylene vinylene)s (OPVs) are attracting ever-increasing interest in the fields of solid-state opto-electronics[1–4] and molecular devices.[5,6] We previously reported that the solid-state molecular packing and fluorescence properties of conjugated linear molecules can be tailored by introducing different side and end functional groups.[7,8] By adopting a similar strategy, we have now synthesized a new type of linear compound which consists of thiomethyl-terminated OPV (TOPV) with methoxyl side groups. This new OPV compound is highly prone to form single crystals. X-ray analysis indicates that it exhibits a rigid planar structure with extended π-conjugated length, which leads to strong solid-state fluorescence induced by absorption of one or two photons. Furthermore, a sharp stimulated emission band is observed to emerge at high excitation intensity in the emission spectrum of TOPV single crystals. The strong two-photon excited fluorescence and stimulated emission are extremely attractive for numerous applications such as light-emitting diodes (LEDs), nonlinear optics, photoconductors, photovoltaics, and upconversion lasing (UCL).[9–14]

The TOPV was synthesized by a one-pot method using a classical Horner–Wadsworth–Emmons coupling reaction (Scheme 1), which is similar to the method used by Bazan et al.[15,16] It readily forms single crystals up to several millimeters long. Figure 1 shows an optical micrograph of a cuboid crystal of TOPV and polarized fluorescence micrographs of the same crystal. The emission is significantly more intense when the crystal is excited with polarization of the excitation light perpendicular to the long axis. The strongly anisotropic fluorescence of the TOPV crystal, which can be clearly observed even with the naked eye, suggests highly anisotropic molecular packing. It is known that the lowest electronic transition ($1A_g \rightarrow 1B_u$) of OPV is optically allowed and polarized mainly along the long molecular axis;[17] hence, Figure 1 reveals that the TOPV molecules are packed such that their long axes mostly lie along the short axis of the crystal. Furthermore, the TOPV crystals show good stability under ambient conditions and even under UV irradiation (Figure S1, Supporting Information), and they exhibit no evidence of efflorescence or changes in fluorescence properties after being stored in liquid paraffin for several months. The solid material is also considerably stable at high temperature, and this allows it to be used in physical vapor deposition

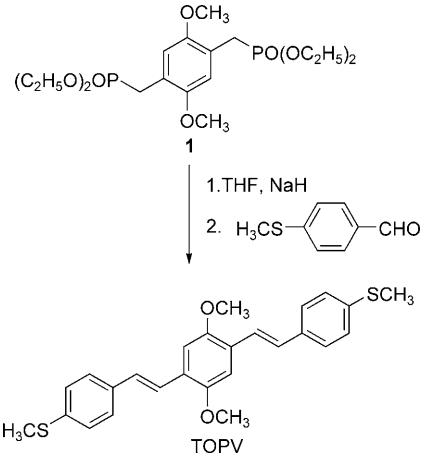

Scheme 1. Synthesis of TOPV.

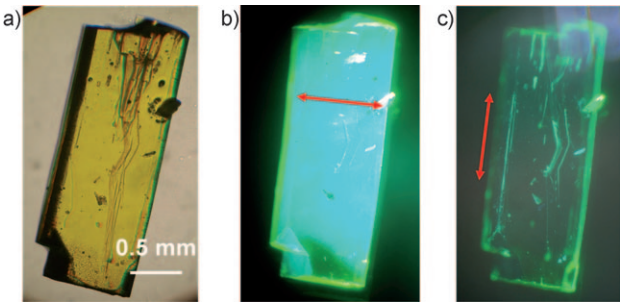

Figure 1. Optical micrograph of a crystal of TOPV (a) and polarized fluorescence micrographs of the same crystal, with polarization angle perpendicular (b) and parallel (c) to the long axis of the crystal (the polarization directions are indicated by arrows).

[*] F. Gao, Z. Z. Xu, Y. H. Yue, Dr. Q. Wang, Prof. H. L. Zhang
State Key Laboratory of Applied Organic Chemistry
College of Chemistry and Chemical Engineering
Lanzhou University, Lanzhou 730000 (P. R. China)
Fax: (+86) 931-891-2365
E-mail: haoli.zhang@lzu.edu.cn
Dr. Q. Liao, Prof. H. B. Fu
Beijing National Laboratory for Molecular Sciences (BNLMS)
Institute of Chemistry Chinese Academy of Sciences
Beijing 100190 (P. R. China)
Fax: (+86) 10-8261-6517
E-mail: hongbing.fu@iccas.ac.cn

[**] This project is supported by National Natural Science Foundation of China (NSFC. 20621091, 20873163, 90606004, 20903051), the Chinese Academy of Sciences ("100 Talents" program), the "111" program, and the National Research Fund for Fundamental Key Project 973 (2006CB806202, 2006CB932101).

Supporting information for this article is available on the WWW under http://dx.doi.org/10.1002/anie.200905428.

to produce highly fluorescent microwires (Figure S2, Supporting Information).

The high fluorescence anisotropy of the TOPV crystal is attributed to its highly anisotropic molecular packing. The X-ray single-crystal structure of this material is depicted by Figure 2a. The crystal structure confirms that the double

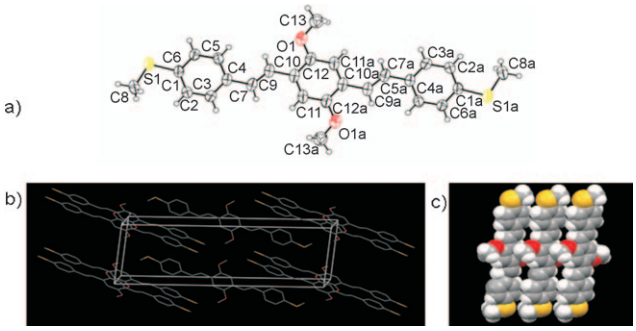

Figure 2. a) Single-crystal X-ray structure of TOPV. Monoclinic crystal system; space group $P21/c$; $a = 8.1520(7)$, $b = 5.4181(4)$, $c = 26.137(2)$ Å, $\beta = 97.374(4)°$. b) Unit cell of TOPV viewed through the *ac* plane. c) Molecular packing along the *b* axis. (CCDC 675387 contains the supplementary crystallographic data for this paper. These data can be obtained free of charge from The Cambridge Crystallographic Data Centre via www.ccdc.cam.ac.uk/data_request/cif.)

bonds in TOPV molecule exist in all-*trans* form. The three benzene rings linked by double bonds are coplanar, and the two thiomethyl groups lie on each side of the plane defined by the aromatic rings with a small dihedral angle of 18.02°. The crystallographic inversion symmetry is coincident with the molecular symmetry.

The crystal structures of various OPV derivatives have been extensively investigated previously.[17,18] It is well understood that the crystals of unsubstituted OPV molecules consist of stacks of basal planes with herringbone intraplane packing, and the strongest interactions exist between the nearest edge-to-face neighbors within the plane, which give so-called H-aggregates.[17] Figure 2b shows a direct view of the arrangement of fluorescent chromophores in the TOPV crystal. The molecules lie parallel to each other with an interplane distance of 3.529 Å, which favors formation of a J-aggregate structure (Figure 2c). In the stack, the long molecular axis is aligned close to the *c* axis, which is tilted 78.55 and 84.67° with respect to the *a* and *b* axes, respectively. The parallel molecular packing is mainly attributed to the steric hindrance introduced by the thiomethyl and methoxyl units. The existence of strong $OCH_3 \cdots \pi$ interaction[19] is evident from the close contact (2.682 Å) between the terminal hydrogen atom on the methoxyl group and the center of the middle ring in the neighboring molecule.

Figure 3 shows the fluorescence excitation and emission spectra of TOPV in dichloromethane solution and in the solid state. The excitation spectrum of TOPV in CH_2Cl_2 solution (Figure 3b) is similar to its absorption spectrum (Figure S3, Supporting Information) with a maximum at 402 nm and a shoulder at 340 nm, and the low-energy tail extends to about 455 nm. In comparison, the diffuse-reflection absorption spectrum of crystal powder is broad and structureless, and

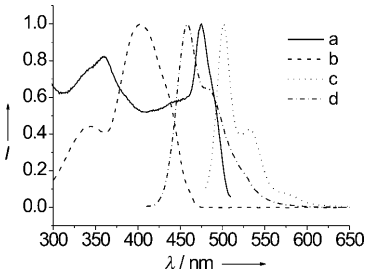

Figure 3. Excitation (a, b) and emission (c, d) spectra of TOPV crystal powder (a, c) and solution in CH_2Cl_2 with a concentration of 5×10^{-6} mol L^{-1} (b, d). The emission spectra of solution and crystal powder were recorded by excitation at 400 and 475 nm, respectively, while the excitation spectra of solution and crystal powder were recorded by monitoring the emission at 460 and 501 nm, respectively.

the low-energy tail extends beyond 520 nm (Figure S3, Supporting Information), in contrast to its excitation spectrum (Figure 3a), which shows a sharp peak at 475 nm. Remarkably, the main emission peak is redshifted from 460 nm in solution to 501 nm in the solid state, though the subband spacing in both solution and crystal-powder emission spectra have similar energies of around 0.14 eV (1130 cm^{-1}). Moreover, the Stokes shift of the crystal powder (1093 cm^{-1}) is only about one-third of that of the solution (3136 cm^{-1}). To obtain further information on the nature of the excited state, we measured the fluorescence lifetimes (Figure S4, Supporting Information). The fluorescence decay of the crystal powder at 501 nm ($\tau_{av} = 0.52$ ns) is much faster than that of the solution at 460 nm ($\tau_{av} = 1.20$ ns). These spectral characteristics observed for the crystal powder as opposed to the solution, that is, red-shifted absorption and emission, smaller Stokes shift, and faster fluorescence decay, are consistent with J-aggregation.[20–23] Note that solid aggregates of unsubstituted OPVs usually display hypsochromic absorption shift and diminished emission at room temperature, which are characteristics of H-aggregation. Although it is not yet fully understood, the solid-state packing of our TOPV molecules concentrates oscillator strength at the bottom of the exciton band (J-aggregate), rather than the top of the exciton band (H-aggregate), as in solids of unsubstituted OPVs.[17,24]

In CH_2Cl_2 solution, TOPV exhibits extremely high fluorescence efficiency with an absolute fluorescence quantum yield close to unity and a relative quantum yield of (96 ± 3) % (9,10-diphenylanthracene in cyclohexane as reference, quantum yield 95 %, excited at 350 nm). Meanwhile, the TOPV crystal displays very strong solid-state fluorescence with a high absolute quantum yield of (41 ± 2) %, higher than those of most reported fluorescent organic crystals. Based on the stereoplot of the unit cell of TOPV, the arrangement in principle favors propagation and emission of excitons in crystalline solids,[14,23] which may hence lead to the intense emission of fluorescent light of TOPV.

Two-photon absorption (TPA) cross sections of TOPV were measured by using a Ti:sapphire laser as the excitation source (Figure 4). It has large TPA cross sections spanning a wide wavelength range between 700 and 800 nm. At 730 nm the TPA has an exceptionally large cross section of 3137 GM (1 GM = 10^{-50} cm^4 s photon^{-1} molecule^{-1}), which is compara-

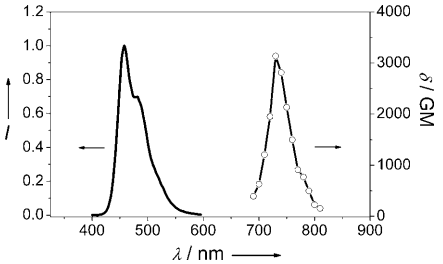

Figure 4. Normalized two-photon-excited fluorescence spectra of TOPV in THF solution at an excitation wavelength of 740 nm (solid lines) and calculated TPA cross sections (circles).

ble to those of perylene derivatives specially designed for applications in optical limiting and UCL.[9] The very broad two-photon excitation window and large TPA cross section of TOPV provide high flexibility in performing investigations and designing photonic devices based on TPA phenomena. As further evidence, the two-photon-excited fluorescence intensity as a function of the incident energy shows a square dependence (Figure S6, Supporting Information), which implies that the upconverted emission indeed stems from the two-photon-absorption mechanism.

Because of the very large TPA cross sections, two-photon-excited fluorescence of TOPV in the solid state can be unambiguously recorded even on a standard spectrofluorimeter with a Xeon lamp as excitation source. As shown in Figure 5, the fluorescence spectra remain the same shape as

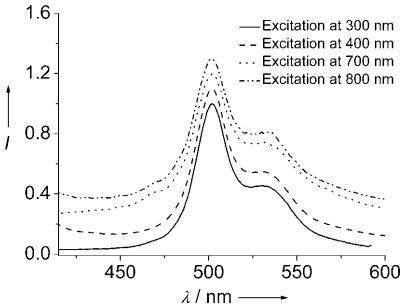

Figure 5. Normalized solid-state fluorescence spectra of TOPV at different excitation wavelengths.

that obtained by one-photon absorption, that is, the same emission processes from the one-photon and two-photon excited states to the ground state are involved. The emission spectra of TOPV in solution, either induced by one-photon or by two-photon absorption, also show similar behavior (Figure S5, Supporting Information).

Interestingly, when a TOPV single crystal ($0.3 \times 0.5 \times 1.0$ mm) was excited at 400 nm, development of a sharp emission band at 501 nm was clearly observed on increasing the pumping energy (Figure 6). The inset plots the dependence on excitation power of the photoluminescence (PL) intensity at 501 nm (empty circles in the inset of Figure 6), which shows a superlinear increase with a threshold around 55 $\mu J\,cm^{-2}$. These spectral features are normally discussed as evidence for amplified stimulated emission or lasing of semiconductor structures. By contrast, the spontaneous

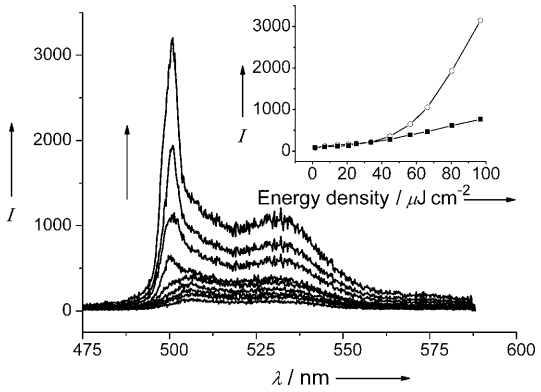

Figure 6. Development of a sharp stimulated emission band with increasing pump intensity (indicated by the arrow) in the emission spectra of a TOPV crystal with excitation at 400 nm. The inset shows the intensity change at 501 (○) and 540 nm (■) at different pump intensities.

emission band at 540 nm continues to increase in a sublinear fashion (filled squares in the inset of Figure 6). We further studied the decay profiles of the PL at 501 nm as a function of pumping energy (Figure S7, Supporting Information). At low excitation intensity, such as 15 $\mu J\,cm^{-2}$, the average lifetime of spontaneous emission is 0.46 ns, and this value slightly decreases with increasing pumping energy. On further power increase above the threshold, to 80 $\mu J\,cm^{-2}$, the lifetime decreases rapidly to an average value of 56 ps. The obviously shortened PL lifetime at high excitation intensity suggests that the PL confined in the single crystal is under resonance and gives the stimulated emission. The emission blue edge observed for the single crystal (Figure 6) is slightly shifted to longer wavelength compared with that observed for the crystal powder (Figure 3), probably due to significant self-absorption in the single crystal. However, the good agreement between the appearance of the stimulated emission band at 501 nm and the emission maximum observed for the crystal powder suggests maximum gain efficiency at 501 nm. This mirrorless lasing phenomenon is likely to be associated with the structural perfection of the single crystal and implies potential of TOPV single crystals as laser media.

In summary, we have reported luminescent organic single crystal of TOPV. Its unique photonic properties including strongly anisotropic solid-state fluorescence, high quantum yield, large TPA cross section, stimulated emission, which, together with its known special electronic characteristics, make this material an exciting candidate for many solid-state opto-electronic applications.

Experimental Section

TPA cross section was determined from two-photon-induced fluorescence with Rhodamine B as a reference. A regenerative amplifier (Spitfire, Spectra Physics) seeded with a mode-locked Ti:sapphire laser (Tsunami, Spectra Physics) generated laser pulses of about 120 fs at a wavelength of 795 nm, which were used to drive an optical parameter amplifier (OPA-800CF, Spectra Physics) to obtain a tunable laser in the range of ca. 690–850 nm. The laser beam was focused into a quartz cuvette having an optical path length of 10 mm. The two-photon-induced fluorescence was collected with a right-

angle geometry and detected with a liquid-nitrogen-cooled charge-coupled device (CCD) detector (SPEC-10-400B/LbN, Roper Scientific) attached to a polychromator (Spectropro-550i, Acton).

Photoluminescence measurements were optically pumped by the second harmonic of a mode-locked Ti:sapphire laser (400 nm wavelength, 120 fs pulse width). The pump laser illuminated a single crystal of TOPV at an incidence angle of 45°, and the light emission was collected along the sample surface normal direction. The PL detector was a streak camera (C5680, Hamamatsu Photonics) attached to a polychromator (C5676, Hamamatsu Photonics). The temporal and spectral resolutions of the detector were 2 ps and 0.2 nm, respectively.

Received: September 28, 2009
Published online: December 22, 2009

Keywords: fluorescence · oligomers · oligo(phenylene vinylene)s · organic crystals · upconversion lasing

[1] R. H. Friend, G. R. W. , A. B. Holmes, J. H. Burroughes, R. N. Marks, *Nature* **1999**, *397*, 121.
[2] B. J. Schwartz, *Annu. Rev. Phys. Chem.* **2003**, *54*, 141.
[3] D. S. Seferos, R. Y. Lai, K. W. Plaxco, G. C. Bazan, *Adv. Funct. Mater.* **2006**, *16*, 2387.
[4] S. Marder, J. Perry, W. H. Zhou, S. M. Kuebler, J. K. Cammack, WO 02/079691A1, **2002**.
[5] W. B. Davis, W. A. Svec, M. A. Ratner, M. R. Wasielewski, *Nature* **1998**, *396*, 60.
[6] J. G. Kushmerick, D. B. Holt, S. K. Pollack, M. A. Ratner, J. C. Yang, T. L. Schull, J. Naciri, M. H. Moore, R. Shashidhar, *J. Am. Chem. Soc.* **2002**, *124*, 10654.
[7] H. Wang, L. Tan, L. J. Wang, F. F. Yin, Z. F. Shi, H. L. Zhang, X. P. Cao, *Chem. Phys. Lett.* **2008**, *461*, 271.
[8] Z. F. Shi, L. J. Wang, H. Wang, X. P. Cao, H. L. Zhang, *Org. Lett.* **2007**, *9*, 595.
[9] S. L. Oliveira, D. S. Corrêa, L. Misoguti, C. J. L. Constantino, R. F. Aroca, S. C. Zilio, C. R. Mendonça, *Adv. Mater.* **2005**, *17*, 1890.
[10] F. He, L. L. Tian, X. Y. Tian, H. Xu, Y. H. Wang, W. J. Xie, M. Hanif, J. L. Xia, F. Z. Shen, B. Yang, F. Li, Y. G. Ma, Y. Q. Yang, J. C. Shen, *Adv. Funct. Mater.* **2007**, *17*, 1551.
[11] M. Albota, D. Beljonne, J. L. Bredas, J. E. Ehrlich, J. Y. Fu, A. A. Heikal, S. E. Hess, T. Kogej, M. D. Levin, S. R. Marder, D. McCord-Maughon, J. W. Perry, H. Rockel, M. Rumi, C. Subramaniam, W. W. Webb, X. L. Wu, C. Xu, *Science* **1998**, *281*, 1653.
[12] J. Kunzelman, M. Kinami, B. R. Crenshaw, J. D. Protasiewicz, C. Weder, *Adv. Mater.* **2008**, *20*, 119.
[13] S. R. Forrest, *Nature* **2004**, *428*, 911.
[14] H. Langhals, O. Krotz, K. Polborn, P. Mayer, *Angew. Chem.* **2005**, *117*, 2479; *Angew. Chem. Int. Ed.* **2005**, *44*, 2427.
[15] H. C. Lin, C. M. Tsai, G. H. Huang, J. M. Lin, *J. Polym. Sci. Part A* **2006**, *44*, 783.
[16] D. S. Seferos, D. A. Banach, N. A. Alcantar, J. N. Israelachvili, G. C. Bazan, *J. Org. Chem.* **2004**, *69*, 1110.
[17] F. C. Spano, *Annu. Rev. Phys. Chem.* **2006**, *57*, 217.
[18] G. P. Bartholomew, G. C. Bazan, X. H. Bu, R. J. Lachicotte, *Chem. Mater.* **2000**, *12*, 1422.
[19] C. M. L. Vande Velde, J. K. Baeke, H. J. Geise, F. Blockhuys, *Acta Crystallogr. Sect. C* **2005**, *61*, o284.
[20] O. J. Dautel, G. Wantz, R. Almairac, D. Flot, L. Hirsch, J. Lere-Porte, J. Parneix, F. Serein-Spirau, L. Vignau, J. J. E. Moreau, *J. Am. Chem. Soc.* **2006**, *128*, 4892.
[21] E. E. Jelley, *Nature* **1936**, *138*, 1009.
[22] G. Scheibe, *Angew. Chem.* **1936**, *49*, 563.
[23] T. Kobayashi, *J-Aggregates*, World Scientific, Singapore, **1996**.
[24] M. Muccini, M. Schneider, C. Taliani, M. Sokolowski, E. Umbach, D. Beljonne, J. Cornil, J. L. Brédas, *Phys. Rev. B* **2000**, *62*, 6296.

